

IAC-13,A6,P,12

SPACE DEBRIS CLOUD EVOLUTION IN LOW EARTH ORBIT

Francesca Letizia

University of Southampton, United Kingdom, f.letizia@soton.ac.uk

Dr. Camilla Colombo*

University of Southampton, United Kingdom, c.colombo@soton.ac.uk

Dr. Hugh Lewis

University of Southampton, United Kingdom, hglewis@soton.ac.uk

Prof. Colin R. McInnes

University of Strathclyde, United Kingdom, colin.mcinnnes@strath.ac.uk

The Earth is surrounded by inoperative objects created by past space missions; as the orbital speed is very high, the impact with a very small fragment, down to 1 cm, can be catastrophic for operating satellites. Therefore, it is important to assess the collision risk due to space debris; this requires a reliable picture of the debris environment and a deep understanding of its evolution. In this work, an analytical approach is used to describe the evolution of a debris cloud created by a collision in Low Earth Orbit. In contrast to traditional approaches, which follow the trajectory of single fragments, here the cloud behaviour is studied globally. This reduces the computational time needed to estimate the consequence of a collision and allows simulating several *what-if* scenarios to understand which objects, in case of fragmentation, are more likely to pose an hazard to operational spacecraft. The NASA break-up model is used to describe fragments dispersion in terms of characteristic length, area-to-mass ratio and velocity. From the velocity distribution the fragment spatial dispersion is derived, through an estimation of the time after which the fragments create a band around the Earth. The cloud density is expressed by a distribution function that depends only on altitude and that is set as initial condition for the orbit propagation. Based on an analytical approach proposed in the literature for interplanetary dust and spacecraft swarms, the fragment cloud evolution in time is derived through the continuity equation. In this application, the continuity equation describes the variation of debris density considering Earth's gravity and atmospheric drag. The cloud evolution is compared to the numerical integration to assess the method's accuracy. The proposed approach proves to be very promising as it is able to capture the main phenomena undergoing the evolution of the semi-major axis distribution. The applicability limits are discussed and the main areas for the method improvement are identified.

I. INTRODUCTION

Space debris is gaining increasing interest by space agencies as it is now clear how its uncontrolled growth could interfere with the exploitation of space, which, on the other hand, has become essential to everyday life¹. Obtaining a reliable picture of space debris environment and understanding the evolution of its orbits are two key-elements to evaluate the consequent risk, to analyse possible mitigation strategies and to suggest future policies.

The prediction of the motion of space debris is quite complex. The objects produced by explosions and collisions, which represent around 60% of the total debris population²¹, have larger area-to-mass ratios than common satellites, so the fragments are

highly affected by the perturbative forces whose intensity depends on the cross-sectional area, such as atmospheric drag and solar radiation pressure³. While such perturbing accelerations are sometime neglected when dealing with satellite motion, they are essential to describe space debris evolution. This means that, while satellite trajectories can be studied using the analytical expression of the two body problem, the analysis of space debris evolution is done using numerical propagation to consider the perturbation effect on each fragment. Moreover, shape, mass and velocity of a fragment generated by a collision or an explosion can be predicted only with high level of uncertainty, so statistical methods (e.g., Monte Carlo method) are required to obtain reliable results¹.

* Currently Marie Curie Research Fellow at Politecnico di Milano, Italy

For these reasons, the simulation of debris population evolution or of the consequence of a fragmentation event can be quite demanding in term of computational time. Semi-analytical methods can be used to accelerate the computation. Given the uncertainty introduced by the mentioned sources, it is unnecessary to compute the fragment trajectories to very high precision, especially as it requires very long simulation time. Instead, it is possible to simplify the model to obtain a faster code, which allows the simulation of a large array of cases and so a deeper insight of the on-going phenomena. The simplification of the propagation is achieved in three ways:

- considering only the most relevant perturbations;
- reducing the number of objects that are actually propagated
- using semi-analytical expression to describe the effect of perturbations.

For example, Rossi et al.⁴ consider only drag and the semi-major axis a and the eccentricity e variations are computed through the analytical expressions derived by King-Hele⁵. The whole debris population is divided into bins of altitude and object size; the number of objects in each bin is used as state variable. Its variation is computed considering the collision/explosion rate for each bin and only one representative element per bin is propagated forward in time to consider the effect of drag on the cloud. Their results are in good agreement with numerical results in Low Earth Orbit (LEO) and the method is able to propagate a cloud of more than 800 objects for 100 years in less than 10 s⁶. Here, semi-analytical methods are used only in the propagation phase as average equations of the dynamics are numerically integrated rather than the full dynamics. Moreover, the fundamental unit of the model is still the single fragment so this kind of methods can be classified as semi-analytical.

A more radical analytical approach is proposed by Valk et al.⁷: the authors write a Hamiltonian formulation for the dynamics of space debris under the effect of gravity potential, luni-solar perturbation, and solar radiation pressure⁸. Drag is not considered, as it is not a conservative force, so this model is not applicable for LEO, but it allows a fast evaluation of the debris population in Geosynchronous Earth Orbit (GEO) region over several hundreds of years.

Similarly, Izzo⁹ proposes a method that describes the debris population globally through the definition of some density functions. In the examples shown^{9,10} the propagation of the population is performed by studying how the density functions in the argument of the periapsis ω and in the longitude of the ascending node Ω change under the effect of the Earth's oblateness. Also

in this case drag is not considered, the method is more suited to describe the GEO region.

However, LEO can be considered as the most crucial area for space debris study. First of all, the density of fragments is much higher in LEO than in GEO and in some regions, e.g. synchronous orbits, it is likely to be very close to the critical value for cascading¹¹, that is the density is so high that the collisions among fragments create much more new objects than the ones that are removed by air drag. Secondly, the International Space Station (ISS) is in LEO and its protection from space debris is essential both for the presence of astronauts and for the delicate experiments, which need to be interrupted in case of collision avoidance manoeuvre¹². Finally, the relative velocity is much higher in LEO than in GEO and so collisions tend to be more dangerous¹³.

This work evaluates the applicability of an analytical method to describe debris motion in Low Earth Orbits. The central idea of the approach is to consider the cloud of fragments generated by a collision globally, as a fluid with continuous properties. The state variable of the system is the cloud density, whose evolution with time, under the effect of the Earth's gravity and perturbations, is obtained through the continuity equation. This approach was applied to describe the evolution of orbital debris population¹⁴, whereas it proved to be effective in describing the motion of interplanetary dust¹⁵, high area to mass ratio spacecraft¹⁶ and nano-satellites constellation.¹⁷

The proposed method requires some simplifying assumption, but the reduced accuracy in predicting the exact position of each fragment is compensated by a more flexible and fast model, that could enable new analysis on the debris population evolution.

II. ANALYTICAL APPROACH

The aim of this work is to develop an analytical method to describe the evolution of the fragment cloud formed by a collision in space. The algorithm to achieve this goal requires the following building blocks, represented in Fig. 1 and described in this section:

- a breakup model, to generate the fragments and their characteristics (i.e., size, mass, velocity) depending on the energy of the collision;
- a model to identify and describe the position of the fragments in the phase when the analytical method becomes applicable (i.e., initial condition for the analytical method);
- a block to transform the information on the fragment positions into a continuous density function;
- an analytical formulation (i.e., the continuity equation) to describe the evolution of the cloud density with time.

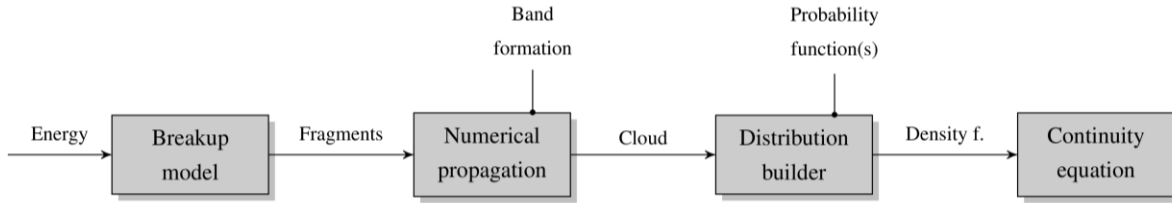


Fig. 1: Algorithm building blocks

Breakup model

A breakup model translates the initial conditions of an explosion or a collision into the characterisation of the generated fragments, in terms of number, size, mass, ballistic coefficient and velocity variation^{18,19}. These parameters, which depend on the energy involved in the fragmentation event and the nature of the event (i.e., collision or explosion), are required to simulate the fragment cloud evolution under the effect of gravity and perturbation forces.

The breakup model adopted in most of the tools for characterising the global evolution of space debris (ORDEM, EVOLVE, MASTER, DAMAGE²⁰) is the NASA breakup model, developed by Johnson¹⁸ and Krisko²¹ and here applied.

The model is here implemented considering non-catastrophic collisions and only the fragments whose size is in the range 1 mm – 8 cm, to avoid the discontinuities present in the model and study how the distributions present in the NASA breakup model influence the fragment dispersion. The maximum ejection velocity is set equal to 1.3 v_c , where v_c is the collision velocity; the ejection velocity direction is random.

Numerical propagation and band formation

Once the fragments are generated and their characteristics defined, the orbital parameters for each fragment orbit are obtained starting from the information on the position and velocity of the fragments. The orbital parameters are propagated numerically using Gauss' equations to compute the effect of atmospheric drag and the Earth's oblateness²².

Drag effect is estimated using an exponential density model

$$\rho = \rho_{ref} \exp\left(-\frac{h - h_{ref}}{H}\right) \quad [1]$$

where the reference values ρ_{ref} and H depend on h_{ref} and are from Vallado²². In the present work, h_{ref} is set as the altitude where the collision occurs and its value is kept constant for the whole simulation; no atmospheric rotation is considered and the maximum altitude below which drag is considered is 1000 km. The variation of

orbital parameters due to drag is computed with the expressions derived by King-Hele⁵ for eccentricity e values between 0.02 and 0.2. Below 0.02 singularities appear, so the fragments whose eccentricity is lower than this threshold are not considered in the propagation or the propagation is stopped. The propagation is stopped also when the perigee altitude h_p is below 50 km as, in this case, the fragment is re-entering through the atmosphere.

Earth's oblateness is included in terms of the long term effect of the zonal harmonic J_2 on the orbital parameters. The implementation of higher order harmonics is not required as the oblateness of the Earth is relevant only for the transition of the cloud shape from a ring to a band around the Earth, which occurs in a period of some months (depending on the parent orbit parameters). Once the band is formed, the argument of periapsis ω , the longitude of the ascending node Ω and the true anomaly ν are randomised in the cloud and so it is not necessary to compute their evolution under the effect of the Earth's oblateness.

The fragment orbital parameters are propagated numerically with semi-analytical methods until they form a *band* around the Earth, under the effect of Earth's gravity and oblateness²³. When the band is formed, the fragment density depends on the distance from Earth only, while the angles ω , Ω , ν are randomised; in these condition, in fact, it is possible to apply the equations developed by McInnes¹⁷ to describe cloud evolution. We are currently working on including also the dependence on ω and Ω in the density, so that the analytical method will be able to describe the cloud evolution starting from only a few revolutions around the Earth.

In literature some analytical expressions to estimate the time required to the fragments to form a band around the Earth are proposed^{24,25,26}; they allow computing the band formation period starting from the orbital parameters of the initial orbit and so they can be used to define a criterion to stop the numerical propagation. However, all these formulations rely on the hypothesis that apsidal and nodal dispersion is complete when the faster fragment, in terms of apsidal/nodal rate, encounters the slowest one. Actually, as explained by

Jehn²³, when the fastest particle meets the slowest one, the fragments are not still uniformly distributed in ω and Ω and so their state cannot be described only as a function of the distance r . As a result, the analytical tend to underestimate the required time.

Therefore, a multiplication factor is introduced. This was computed comparing the distribution of the angles (ω , Ω , ν) with a uniform distribution between $-\pi$ and π , through the Kolmogorov-Smirnov test²⁶: the band is considered formed at the time when the hypothesis of uniform distribution becomes acceptable. In the following results the formulation by Ashenberg²⁶ is used

$$T_{\Omega} = \frac{\pi}{3J_2 \frac{R_E^2}{a^3} (7 \cos i \cos \beta + \sin i \cos u \sin \beta) \delta \nu}$$

with

$$\tan \beta = \frac{1}{7} \tan i \cos u$$

where R_E is the Earth's radius, a is the semi-major axis, i is the inclination, u is the longitude of the periaspis, $\delta \nu$ is the (average) variation of the velocity due to the fragmentation event; a multiplication factor of 2 is applied.

Position fitting

Once the band is formed, the numerical integration is stopped and the information on the fragment orbital parameters has to be converted in a continuous function that describes the fragment density and that will be used as initial condition for the analytical propagation.

The position fitting is performed through the parametric approach, where it is assumed that the functional form of the fitting function is known and only some parameters need to be calculated²⁶. Some standard distribution functions were tested and their fitness was evaluated through the quantile-quantile plot (Fig.2) and the Kolmogorov-Smirnov statistic, which measures the maximum distance between the empirical cumulative distribution function of the (simulation) data and the cumulative distribution function used to fit the data (Fig.3).

In particular, the latter approach allows quantifying the fitness of all the tested distribution functions as summarised in Table 1 and so it provides a criterion to rank them; as a result, the algorithm is able to choose the best function for each application.

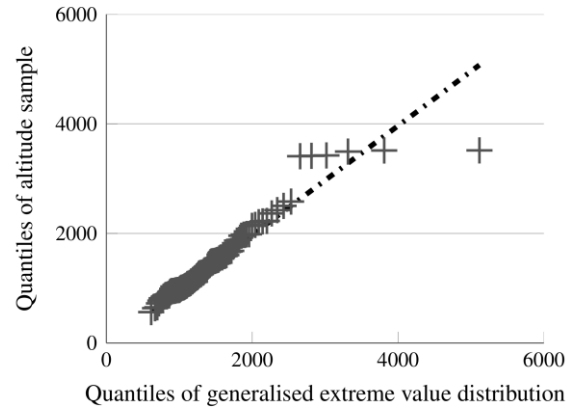


Fig.2: Quantile-quantile plot of the generalised extreme value in case of a fragmentation event at 800 km

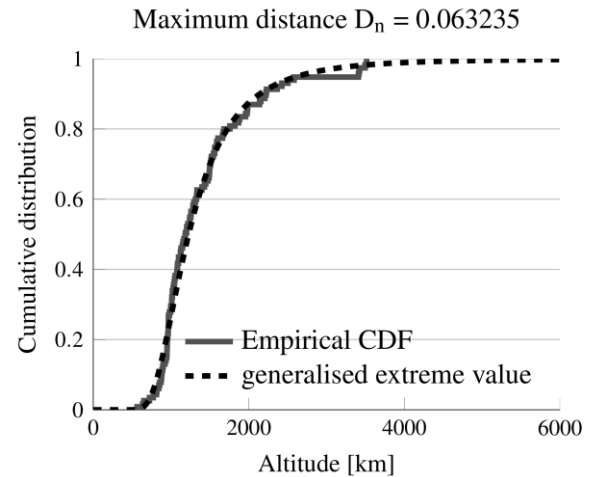


Fig.3: Empirical cumulative distribution function plotted against the generalised extreme value cumulative distribution function

Distribution	KS	Distribution	KS
Birbaum-Saunders	0.1038	Log-normal	0.0990
Extreme value	0.2373	Nagakami	0.1546
Gamma	0.1225	Normal	0.1688
Generalised extreme value	0.0632	Rayleigh	0.1986
Inverse gaussian	0.1022	Rician	0.1984
Logistic	0.1368	T location scale	0.1404
Log-logistic	0.0804	Weibull	0.1511

Table 1. Value of the Kolmogorov-Smirnov statistic for the tested distribution functions

The function used to fit the semi-major axis distribution is the *generalised extreme value*, whose cumulative distribution function is

$$F(x; \mu, \sigma, \xi) = \exp \left\{ - \left[1 + \xi \left(\frac{x - \mu}{\sigma} \right) \right]^{\frac{1}{\xi}} \right\},$$

where μ is the location parameter, σ is the scale parameter, which indicates how spread the distribution is, and ξ is the shape parameter, which indicates if the distribution is symmetric or not.

Analytical propagation

Once the initial fragment density is defined, the continuity equation is used to analytically derive the evolution of density n with time and altitude.

The continuity equation can be written as

$$\frac{\partial n}{\partial t} + \nabla \cdot \mathbf{f} = \dot{n}^+ - \dot{n}^- \quad [2]$$

and at the moment, no discontinuous events are considered, so $\dot{n}^+ - \dot{n}^- = 0$; the term $\nabla \cdot \mathbf{f}$ models the continuous phenomena and in this case drag is considered, following the approach developed by McInnes¹⁷.

A spherically symmetrical initial condition is considered and the drift velocity in the radial direction v_r depends only on drag effect. The radial velocity v_r is obtained starting from the expression of drag acceleration

$$a_D = \frac{1}{2} \frac{c_D A}{M} \rho(r) v^2 \quad [3]$$

where c_D is the drag coefficient of the fragment, which is supposed to be constant and equal to 2.2²²; A is the fragment cross-sectional area; M is the fragment mass; v is the fragment velocity and $\rho(r)$ is the atmosphere density, which depends on the distance from the Earth. The term $\rho(r)$ is expressed through the exponential model in Equation [1] and the parameter ε is introduced

$$\varepsilon = \sqrt{\mu} \frac{c_D A}{M} \rho_{ref} \exp \left(\frac{h_{ref}}{H} \right).$$

Applying the method of characteristics, McInnes¹⁷ obtains an explicit expression for the density evolution

$$\log \{n(r, t)\} = \log \{-\varepsilon r^{5/2} \exp[-r/H]\}^{-1} + \Psi \{ \exp[r/H] + (\varepsilon \sqrt{R_H} / H) t \}. \quad [4]$$

where the function Ψ is obtained from the initial distribution $n(r, t = 0)$

$$\begin{aligned} \Psi(z) &= \log \{n(r, 0)\} - \log \{r^2 v_r(r)\}^{-1} \\ &= \log \{n(H \log z)\} + \log \{-\varepsilon z^{-1} (H \log z)^{5/2}\} \end{aligned} \quad [5]$$

with the independent variable $z = \exp[r/H]$.

Here, three important observations should be done. Firstly, Equation [4] provides a fully analytical expression to compute the effect of drag on the cloud and the analytical propagation always acts on the cloud globally, not on the single fragments. Secondly, Equation [5] shows that the initial fragment density can be described with any explicit function, as no particular operation is done on the function $n(r, t = 0)$.

Finally, it is important to observe that in this formulation the shape of the initial condition is used only as a starting point for the analytical method, which is able to modify the function shape to follow the evolution of cloud. To demonstrate this point, let's consider to model the initial condition with a normal distribution

$$n(r, 0) = n_m \exp[-\lambda(r - r_m)^2]$$

and to write explicitly the expression of $n(r, t)$ given by Equation [4]

$$\begin{aligned} n(r, t) &= n_m \exp \left\{ -\lambda \left[H \ln \left(\exp \left[\frac{r}{H} \right] + \varepsilon \frac{\sqrt{R_H}}{H} t \right) - r_m \right]^2 \right\} \\ &\cdot \left[H \ln \left(\exp \left[\frac{r}{H} \right] + \varepsilon \frac{\sqrt{R_H}}{H} t \right) - r_m \right]^{5/2} \\ &\cdot \frac{1}{\exp \left[\frac{r}{H} \right] + \varepsilon \frac{\sqrt{R_H}}{H} t}. \end{aligned} \quad [6]$$

Introducing

$$\tilde{z} = H \ln \left(\exp \left[\frac{r}{H} \right] + \varepsilon \frac{\sqrt{R_H}}{H} t \right)$$

the Equation [6] becomes

$$n(\tilde{z}) = n_m \exp[-\lambda(\tilde{z} - r_m)^2] \frac{\tilde{z}^{5/2}}{\exp[\tilde{z}/H]} \quad [7]$$

and one can observe that the shape of the initial condition $n_m \exp[-\lambda(\tilde{z} - r_m)^2]$ is modified by the factor $\frac{\tilde{z}^{5/2}}{\exp[\tilde{z}/H]}$ that depends on the dynamics of the problem.

III. PRELIMINARY RESULTS

The method described in Section II is implemented and compared to the traditional numerical integration of the trajectory of each fragment.

The parent orbit before the collision is here considered to be circular and planar; its altitude is set to 800 km as it is the altitude where the density of space debris is the highest¹¹.

A non-catastrophic collision is here considered, with projectile mass equal to 100 g and collision velocity of 1 km/s: the collision generates more than 2000 fragments whose orbital parameters are numerically propagated up to band formation, set at a number of orbits double of the value predicted by Ashenberg²⁶. The numerical propagation was performed in Keplerian elements by means of Gauss' equations averaged on the orbital period²². When the band is formed, the distribution of the semi-major axis a is used to build the initial condition for the fragment density in terms of altitude.

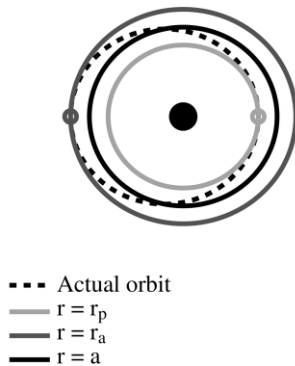


Fig. 4: Diagram of nominal orbit and different circular approximations: perigee radius r_p , apogee radius r_a , semi major axis a . In this example the eccentricity e is equal to 0.2.

Since the analytical method assumes that the orbits are circular, choosing the semi-major axis as independent variable allows saving the information on the orbit energy.

If, instead, the initial condition was built from the fragment positions, this would imply that the analytical method approximates the actual orbit family with circular ones using as a reference radius the distance measured at the time of band formation; if the eccentricity is very low, the error introduced is low; however, as the eccentricity increases, the difference in energy becomes noticeable.

In Fig. 4 the comparison between the actual orbit and different circular approximations is shown. If the value of the perigee r_p is used, the obtained circular orbit (light grey curve) is much lower in altitude than the actual one, so the effect of drag will be much amplified; on the other hand, using the radius at the apogee r_a (dark grey curve) the decay due to atmosphere is underestimated. As the particles are slower close to the apogee, it is likely that *more* fragments are close to the apogee²⁸. The semi-major axis provides an average value for the radius and it also allows saving the information on the orbit energy. For this reason, the value of semi-major axis is used and compared both to the actual distribution of fragment distance and semi-major axis.

Single area-to-mass ratio

Fig. 5 shows the comparison between the numerical and the analytical method in terms of semi-major axis distribution at different times; the numbers above each plot indicate the number of days since the band formation.

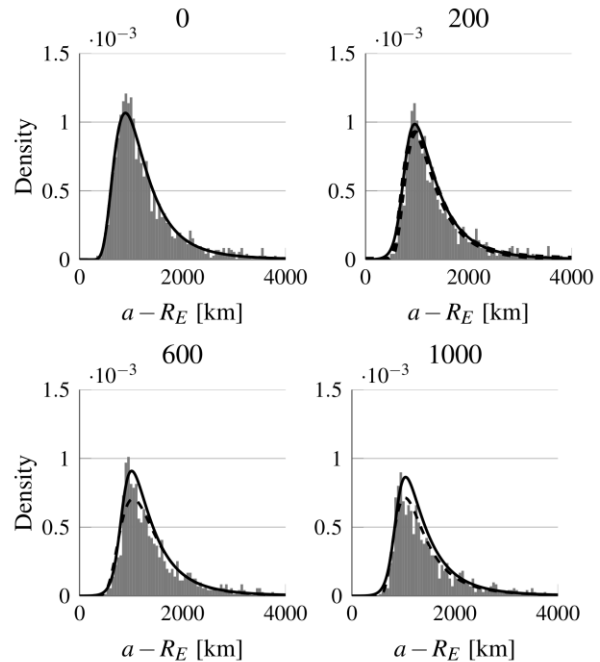


Fig. 5: Evolution of the cloud density in term of semi-major axis a . The numbers above each graph indicate the number of days since the band formation. The solid line represents the results of the analytical method, the dashed line the fit of the distribution obtained with the numerical propagation.

The histograms represent the distribution of fragments according to the numerical propagation and the density of fragments at the time j in the k^{th} bin is computed as

$$n_{j,k} = \frac{N_{j,k}}{h_k N_{tot}}$$

where $N_{j,k}$ is the number of fragment at a specific altitude divided by the total number of fragment at the band formation N_{tot} and the width of the altitude bins h_k . The solid curve represents the distribution obtained with the analytical method, as in Equation [4], and the dashed curve represents the fit of the numerical results done with the best fitting distribution function (i.e., the *generalised extreme value*) used to set the initial condition for the analytical method. In this case, it is assumed that all the fragments have the same area-to-mass ratio, which is equal to 0.5 m²/kg.

The first observation is that the numerical fit (dashed curve) is not able to follow the actual evolution of the cloud. This is because the shape of the fragment distribution changes with time and fitting with the same distribution function (in this case the *generalised extreme value*) does not capture this change; for example, it is possible to note that the Kolmogorov-Smirnov statistic increases with time, going from 0.0234 at the band formation to a maximum of 0.0439 after 600 days (Fig. 6). On the other hand, the analytical curve changes with time as the continuity equation does not act on the parameters of the fitting function, but it modifies the function shape as explained in Section II.

It is also possible to observe that the analytical propagation is able to represent the two main undergoing phenomena: the reduction of the fragment number and the shift of the peak toward higher altitude.

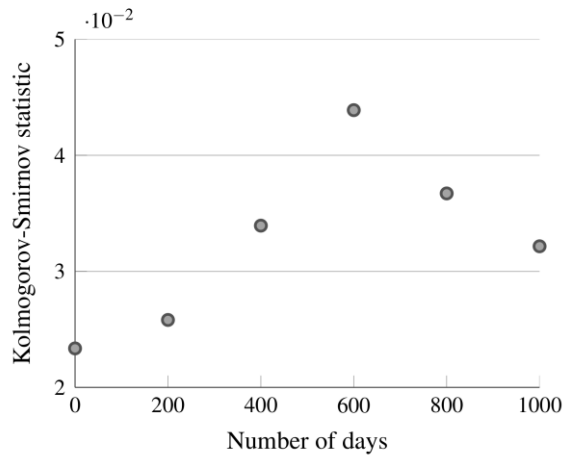


Fig. 6: Evolution of the Kolmogorov-Smirnov statistic for the fit of the numerical data

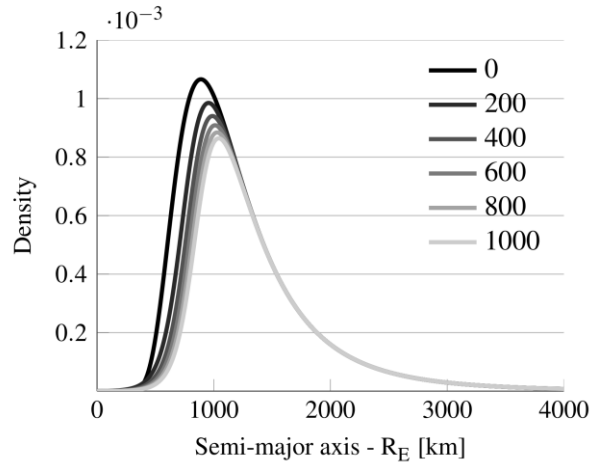


Fig. 7 Evolution of fragment density as computed by the analytical model

The height of the peak is well captured by the analytical method, while the shift of its location is over predicted. This is due to the shape of the initial condition and so the results may be probably improved using a better fitting for the initial condition. This is also visible in Fig. 7 that shows the history of the density obtained with the analytical model.

The comparison between the numerical and the analytical propagation can be done observing also the histograms obtained with the two methods and their difference.

In Fig. 8 the dark grey histograms refer to the numerical propagation and the light grey are representative of the analytical method; the histograms at the bottom express the difference between the two. From the graph at the time of band formation one can observe the initial error due to the incorrect representation of the peak, whose altitude is underestimated of around 12%.

The error is computed as

$$err_i = \frac{\sum_{k=1}^m |\hat{a}_k - \hat{n}_k|}{\sum_{k=1}^m \hat{n}_k},$$

Where \hat{a} and \hat{n} represent, respectively, the histogram estimation of the analytical and the numerical propagation so that \hat{a}_k and \hat{n}_k are the values of density in the k^{th} bin and m is the total number of bins.

The error err_i is equal to 0.1472 at the band formation and grows up to 0.3105 after 1000 days; at this time the error is mainly due to the overestimation of particles at high altitude (>1000 km).

This behaviour can be explained observing the relationship between eccentricity e and semi-major axis a presented in Fig. 9: the fragments with large semi-major axis have also large eccentricity values, so the altitude of perigee is lower than 1000 km and drag affects the fragment while they are close to the perigee, reducing the energy and so the semi-major axis of the orbit. However, in the analytical method the orbits are approximated with circular orbit whose radius is equal to the semi-major axis; as the semi-major axis of these fragments is well above 1000 km, no drag effect is computed. Modelling the dependence of the semi-major axis on the eccentricity will improve the results. This will be done in a future work.

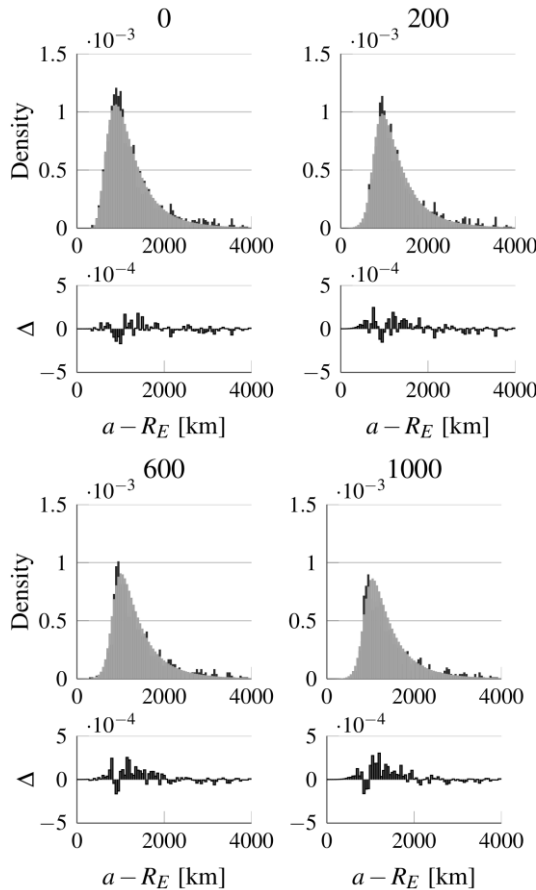


Fig. 8 Comparison between the actual distribution of fragment semi-major axis (dark grey histograms) and the one obtained with the analytical method (light grey histograms); the histogram at the bottom represents their difference. The numbers above each graph indicate the number of days after the band formation.

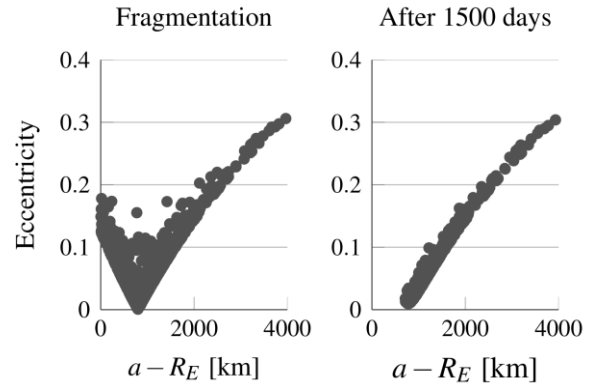


Fig. 9: Eccentricity e values plotted against semi-major axis a at different times of cloud evolution

If the initial condition built on the distribution of the semi-major axis is used to predict the distribution of the fragment altitude the results are less accurate: as shown in Fig. 10, the initial condition (solid curve) is not able to correctly represent the initial distribution, as the peak height is not captured; during the cloud evolution the two methods agree on the reduction of the fragment number, but the distribution obtained are quite different. Also in this case, modelling the effect of eccentricity distribution can improve the results.

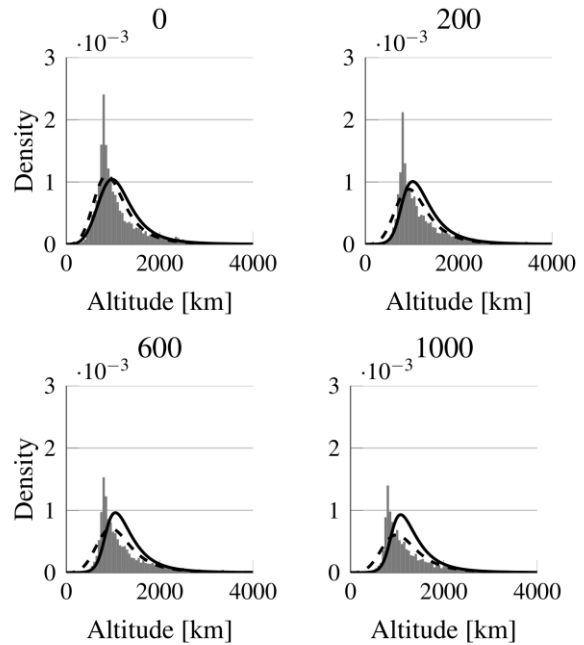


Fig. 10: Evolution of the cloud density in term of distance r . The numbers above each graph indicate the number of days since the band formation. The solid line represents the results of analytical method, the dashed line the fit of the distribution obtained with the numerical propagation.

Multiple values of area-to-mass ratio

If the complete NASA model is used, the cloud is formed by fragments with different values of area-to-mass ratio. If the analytical propagation is obtained using an average value for the area-to-mass ratio, the method is not accurate enough to describe the cloud evolution.

An alternative approach consists in defining n bins in area-to-mass ratio (currently $n = 5$) and treating each bin with a single (average on the bin) area-to-mass ratio value and then summing the resulting density curves. As shown in Fig. 11, the method is able to deal also with multiple values of area-to-mass ratio.

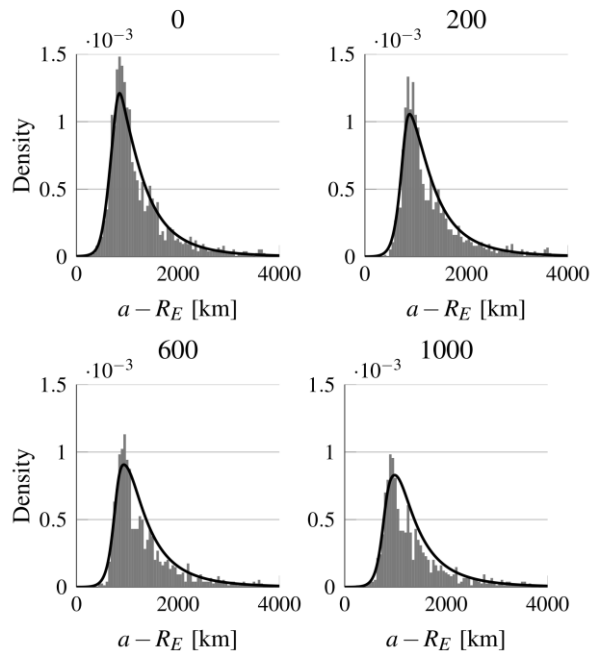


Fig. 11 Evolution of the cloud density in term of semi-major axis a . The numbers above each graph indicate the number days since the band formation. Multiple values of area-to-mass ratio are considered.

Computational time

The numerical and the analytical method can be compared in terms of the computational time required to simulate a certain period of cloud evolution. The result of the comparison is shown in Fig. 12: a cloud of 8000 fragments was studied for 1500 days after the fragmentation event and the measured times refer to a machine with 8 CPUs at 3.40 GHz.

The breakup model requires only 0.1 s to generate the cloud; this is required in both numerical and analytical approaches. Then, the numerical propagation up to band formation lasts around 500 s and it is evident

that this is the main contribution for the computational time of the analytical method.

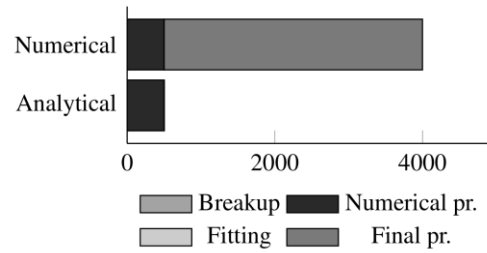


Fig. 12: Computational time in seconds on a machine with 8 CPUs at 3.40 GHz

In fact, in the analytical approach, the curve fitting takes 2.5 s, whereas the computational time of the propagation with the continuity equation is negligible. On the other hand, if the semi-analytical numerical method is used, the simulation of the cloud evolution after the band formation requires more than 3000 s. Moreover, the computational time of numerical propagation depends on the length of the simulation and the number of fragments, while the time for the analytical propagation is always negligible.

This suggests that the analytical method can enable many analyses on the debris population, for example simulating several collisions to understand under which conditions the risk for operating satellites is higher and which objects are more dangerous if involved in a fragmentation event. This will be shown in a future work.

IV. CONCLUSIONS

The study of the consequences of a collision between objects in space is a complex task because of the large number of produced fragments and the relevance of perturbing forces, which are usually neglected when dealing with satellite motion.

In this work, an analytical approach to model fragmentation events in space is developed. The proposed method shifts the focus from the computation of the single fragment trajectories to the study of the global evolution of the fragment cloud. The starting point for the method is a standard fragmentation model, which provides the main features of the fragments generated by the collision; the fragment orbital parameters are numerically propagated until their distribution is spherically symmetrical and it depends only on the distance from the Earth. Then, a continuous function is introduced to describe the fragment density, basically considering the fragment cloud as a fluid with continuous properties. The evolution of the cloud density with time is obtained through the continuity

equation; it is then possible to derive an analytical expression for the fragment density as a function of time.

The current preliminary implementation of the method shows already some interesting and promising results as it is able to model the main changes in the fragment semi-major axis distribution under the effect of drag. This approach can be therefore applied to model collisions in Low Earth Orbit up to 1000 km, where drag is the main perturbing force, which is an extremely important area for space exploitation.

Improving how the eccentricity and area-to-mass ratio are treated will increase the accuracy of the method, making it a suitable model for dealing with space debris risk estimation. This will be implemented in a future work.

In fact, as the proposed approach allows a remarkable reduction of the computational time to

simulate the consequence of a collision, it can enable new analysis on the debris population; for example it can be used to test several different fragmentation scenarios to assess the stability and the criticality of the current debris population.

V. ACKNOWLEDGEMENT

Francesca Letizia is supported by the Amelia Earhart Fellowship for the academic year 2013/2014. The authors acknowledge the use of the IRIDIS High Performance Computing Facility, and associated support services at the University of Southampton, in the completion of this work

-
- ¹ H. Klinkrad, P. Beltrami, S. Hauptmann, C. Martin, H. Sdunnus, H. Stokes, J. Wilkinson. "The ESA space debris mitigation handbook 2002." *Advances in Space Research* 34.5 (2004): 1251-1259.
 - ² P. Krisko. The predicted growth of the low-Earth orbit space debris environment: an assessment of future risk for spacecraft. *Proceedings of the Institution of Mechanical Engineers, Part G: Journal of Aerospace Engineering*, 221 (6):975–985, January 2007. ISSN 0954-4100. doi: 10.1243/09544100JAERO192.
 - ³ C. Colombo and C. McInnes. Orbital Dynamics of "Smart-Dust" Devices with Solar Radiation Pressure and Drag. *Journal of Guidance, Control, and Dynamics*, 34(6):1613–1631, May 2011. doi: 10.2514/1.52140
 - ⁴ A. Rossi, A. Cordelli, and C. Pardini. Modelling the space debris evolution: Two new computer codes. *Advances in the Astronautical Sciences-Space Flight Mechanics*, pages 1–15, 1995.
 - ⁵ D.G. King-Hele. *Satellite orbits in an atmosphere: theory and application*. Blackie, Glasgow and London, 1987. ISBN 0216922526, pagg. 47-55.
 - ⁶ A. Cordelli, P. Farinella, and A. Rossi. Study on long term evolution of Earth orbiting debris. Study note of work package 3200, ESA/ESOC Contract No. 10034/92/D/IM(SC): "Study on Long Term Evolution of Earth Orbiting Debris", 1995.
 - ⁷ S. Valk, A. Lemaître, and F. Deleflie. Semi-analytical theory of mean orbital motion for geosynchronous space debris under gravitational influence. *Advances in Space Research*, 43(7):1070–1082, April 2009. doi: 10.1016/j.asr.2008.12.015.
 - ⁸ S. Valk, N. Delsate, a. Lemaître, and T. Carletti. Global dynamics of high area-to-mass ratios GEO space debris by means of the MEGNO indicator. *Advances in Space Research*, 43(10):1509–1526, May 2009. doi: 10.1016/j.asr.2009.02.014.
 - ⁹ D. Izzo. Statistical modelling of orbits and its application to trackable objects and to debris clouds. PhD thesis, La Sapienza, 2002.
 - ¹⁰ D. Izzo and C. Valente. A mathematical model representing the statistical properties of sets of orbits. *Acta Astronautica*, 54(8):541–546, April 2004. doi:10.1016/S0094-5765(03)00224-8.
 - ¹¹ J.C. Liou. An active debris removal parametric study for LEO environment remediation. *Advances in Space Research*, 47(11):1865 – 1876, 2011. doi: 10.1016/j.asr.2011.02.003.
 - ¹² J.L Foster. The analytic basis for debris avoidance operations for the International Space Station. In *Third European Conference on Space Debris*, pages 441–445, Darmstadt, 2001. ESA Publication Division.
 - ¹³ V. Chobotov. *Orbital mechanics*. American Institute of Aeronautics and Astronautics, Reston, 3rd edition, 2002. ISBN 1563475375.
 - ¹⁴ C.R. McInnes. An analytical model for the catastrophic production of orbital debris. *ESA Journal*, 1993.
 - ¹⁵ N.N. Gor'kavyi. A new approach to dynamical evolution of interplanetary dust. *The Astrophysical Journal*, 474(1):496–502, 1997.

- ¹⁶C. Colombo and C.R. McInnes. Evolution of swarms of smart dust spacecraft. In *New Trends in Astrodynamics and Applications VI*, New York, JUN 2011. Courant Institute of Mathematical Sciences.
- ¹⁷C.R. McInnes. Simple analytic model of the long term evolution of nanosatellite constellations. *Journal of Guidance Control and Dynamics*, 2000.
- ¹⁸N.L. Johnson and P.Krisko. NASA's new breakup model of EVOLVE 4.0. *Advances in Space Research*, 28(9):1377–1384, 2001.
- ¹⁹D. McKnight. Determination of breakup initial conditions. *Journal of Spacecraft and Rockets*, 28(4):470–477, July 1991. doi: 10.2514/3.26268.
- ²⁰H. Sdunnus, P. Beltrami, H. Klinkrad, M. Matney, A. Nazarenko, and P. Wegener. Comparison of debris flux. *Advances in Space Research*, 34(5):1000–1005, January 2004. doi: 10.1016/j.asr.2003.11.010.
- ²¹P. Krisko. Proper Implementation of the 1998 NASA Breakup Model. *Orbital Debris Quarterly News*, 15(4):1–10, 2011.
- ²²D.A. Vallado. *Fundamentals of astrodynamics and applications*. Springer, 2001, pagg 511-541.
- ²³R. Jehn. Dispersion of debris clouds from In-orbit fragmentation events. *ESA Journal*, 15(1):63–77, 1991.
- ²⁴V. Chobotov. Dynamics of orbiting debris clouds and the resulting collision hazard to spacecraft. *Journal of the British Interplanetary Society*, 1990.
- ²⁵D. McKnight. A phased approach to collision hazard analysis. *Advances in Space Research*, 10(3-4):385–388, January 1990. doi:10.1016/0273-1177(90)90374-9.
- ²⁶J. Ashenberg. Formulas for the phase characteristics in the problem of low-Earth-orbital debris. *Journal of Spacecraft and Rockets*, 31(6):1044–1049, November 1994. doi: 10.2514/3.26556.
- ²⁷J.E. Gentle. *Elements of computational statistics*. Springer, 2002.
- ²⁸C.R. McInnes and C. Colombo. Wave-like patterns in an elliptical satellite ring. *Journal of Guidance, Control, and Dynamics*, 2013.